

Selecting an Advanced Creep Model or a Sophisticated Time-Integration? A new Approach by means of Sensitivity Analysis

Holger Keitel

Abstract—The prediction of long-term deformations of concrete and reinforced concrete structures has been a field of extensive research and several different creep models have been developed so far. Most of the models were developed for constant concrete stresses, thus, in case of varying stresses a specific superposition principle or time-integration, respectively, is necessary. Nowadays, when modeling concrete creep the engineering focus is rather on the application of sophisticated time-integration methods than choosing the more appropriate creep model. For this reason, this paper presents a method to quantify the uncertainties of creep prediction originating from the selection of creep models or from the time-integration methods. By adapting variance based global sensitivity analysis, a methodology is developed to quantify the influence of creep model selection or choice of time-integration method. Applying the developed method, general recommendations how to model creep behavior for varying stresses are given.

Keywords—concrete creep models, time-integration methods, sensitivity analysis, prediction uncertainty.

I. INTRODUCTION

THE prediction of long-term deformations of concrete and reinforced concrete structures has been a field of extensive research for many decades and several different creep models have been developed so far. These models vary in their theory, complexity, and in described phenomena. Consequently, the prediction quality of these models varies strongly. Nevertheless, most of these models were developed for constant concrete stresses only, thus, in case of varying stresses a specific superposition principle or time-integration, respectively, is necessary. Different complex time-integration methods exist [1] in order to simulate creep at varying concrete stresses using the models developed for constant stresses. Starting from the simplified Effective Modulus Method, neglecting all stress history and taking only into account the actual material properties and stress state, and ending up in the time and computational power demanding superposition principle by Boltzmann [2] or its extension to non-linear creep by Diener [3].

Analyzing practical applications it is observed that the focus of the engineer is rather on the use of a sophisticated time-integration methods than on the selection of a more appropriate creep model [4]. This occurs even when the codes give the opportunity to choose different creep models and evaluation methods for the prediction quality of these models exist

H. Keitel is a member of the Research Training Group 1462 - "Evaluation of Coupled Numerical Partial Models in Structural Engineering (GRK 1462)" - at the Bauhaus-Universität Weimar, Berkaer Str. 9, 99423 Weimar, Germany (phone: +49-3643-584113, e-mail: holger.keitel@uni-weimar.de).

[5]. For this reason, the present paper presents a method to quantify the uncertainties of creep prediction coming from the selection of creep models or from the choice of time-integration methods by means of sensitivity analysis. From the outcome of exemplary applications of the developed methodology, recommendations for the engineers how to model creep behavior for varying stresses are given.

In the next section the different creep models and time-integration methods are explained. Section III describes the proposed method of variance based global sensitivity analysis followed by a numerical example in order to demonstrate the functionality of the algorithm. Finally, conclusion are drawn from the results of the analyses.

II. CREEP MODELS

A. Creep Models

The applied models are briefly explained in this section. The following equations are only valid for the determination of the creep compliance C_c and creep strain $\varepsilon_{c,cr}$, respectively, for constant stresses. The application of these models to varying stresses is content of the next subsection.

Model ACI209 [6] assumes an ultimate creep coefficient $\varphi_{c,\infty}$ and combines it with a hyperbolic time-function in order to determine the creep compliance C_c . The values of $d = 10$ d for the addend and $\psi = 0.6$ for the exponent of the time-function are recommended. The coefficient $\varphi_{c,\infty}$ is defined by the corrections factor γ_c , depending on concrete age at beginning of loading t_0 , relative humidity RH , concrete composition, geometry, and fresh and hardened concrete properties. The creep coefficient refers to Young's modulus of the concrete age at beginning of loading E_{c,t_0} . The creep compliance C_c becomes

$$C_c(t, t_0) = \frac{\varphi_c(t, t_0)}{E_{c,t_0}} = \frac{\frac{(t-t_0)^\psi}{d+(t-t_0)^\psi} \varphi_{c,\infty}(t_0)}{E_{c,t_0}}. \quad (1)$$

with

$$\varphi_{c,\infty}(t_0) = 2.35 \gamma_c = 2.35 \gamma_{t_0} \gamma_{RH} \gamma_a \gamma_V / S \gamma_{sl} \gamma_f - a. \quad (2)$$

The time-dependent total compliance of concrete J_c additionally includes the elastic compliance and is defined as

$$J_c(t, t_0) = \frac{1}{E_{c,t_0}} + C_c(t, t_0). \quad (3)$$

The resulting creep strain $\varepsilon_{c,cr}$ becomes

$$\varepsilon_{c,cr}(t, t_0) = C_c(t, t_0) \sigma_c \quad (4)$$

and the total strain $\varepsilon_{c,tot}$ is defined as

$$\varepsilon_{c,tot}(t, t_0) = J_c(t, t_0) \sigma_c. \quad (5)$$

Model MC10 [7] is quite similar to ACI209. The differences between both models are the definition of the ultimate creep coefficient $\varphi_{c,\infty}$, referring to Young's modulus at concrete age of 28 days $E_{c,28}$, and the hyperbolic time-function with the exponent of 0.3. Furthermore, an over-proportionality factor $F_\Omega(\sigma_c)$ for stress levels exceeding $0.45f_{cm}$ is integrated in $\varphi_{c,\infty}$. The creep coefficient depends on concrete strength, relative humidity and type of cement. The creep compliance results to

$$C_c(t, t_0, \sigma) = \frac{\varphi_c(t, t_0, \sigma)}{E_{c,28}}, \quad (6)$$

with

$$\varphi_c(t, t_0, \sigma) = F_\Omega(\sigma_c) \varphi_{RH} \beta_{f_{cm}} \beta_{t_0,eff} \left[\frac{t - t_0}{\beta_H + (t - t_0)} \right]^{0.3}. \quad (7)$$

The definitions of the total compliance and strains are equivalent to Eq. (3), (4) and (5).

Similar to MC10 model GL2000 [8] defines the increase of the creep compliance using the creep coefficient φ_c and referring to $E_{c,28}$, Eq. (6). The value of φ_c is defined by humidity, cement type and geometrical properties. In contrast to the first models no ultimate creep coefficient is assumed, rather a continuous increase of creep compliance over time is simulated. The time-dependent development of C_c is defined by hyperbolic and hyperbolic-exponential functions. The factor $\phi(t_c)$ takes into account drying before loading.

$$\begin{aligned} \varphi_c(t, t_0) = & \\ & \phi(t_c) \left[2 \left(\frac{(t - t_0)^{0.3}}{(t - t_0)^{0.3} + 14} \right) + \left(\frac{7}{t_0} \right)^{0.5} \left(\frac{t - t_0}{t - t_0 + 7} \right)^{0.5} \right] \\ & + \phi(t_c) \left[2.5 (1 - 1.086RH^2) \left(\frac{t - t_0}{t - t_0 + 0.15 \left(\frac{V}{S} \right)^2} \right)^{0.5} \right]. \end{aligned} \quad (8)$$

Eq. (3), (4) and (5) hold for the determination of J_c and the strains.

Model B3 [9] is the creep model with the highest physical background, based on the solidification theory by Bažant and Prasannen [10], [11]. It distinguishes creep explicitly into basic and drying creep. Model B3 utilizes the total compliance J_c instead of creep compliance C_c , defined as the following:

$$J_c(t, t_0, \sigma) = q_1 + F_\Omega(\sigma_c) C_0(t, t_0) + F_\Omega(\sigma_c) C_d(t, t_0, t_d), \quad (9)$$

where q_1 is the instantaneous compliance, C_0 is the basic creep compliance, described by the aging visco-elastic compliance q_2 , the non-aging visco-elastic compliance q_3 , and the visco-plastic compliance q_4 , and C_d is the drying creep compliance, defined by q_5 . The parameters $q_1 \dots q_5$ depend on the concrete composition, concrete stiffness and strength, and relative humidity. Over-proportionality for higher stress levels is taken into account by $F_\Omega(\sigma_c)$. In contrast to the other three models the time-independent compliance q_1 is defined by $0.6/E_{c,t_0}$ instead of $1/E_{c,t_0}$. This effectively separates

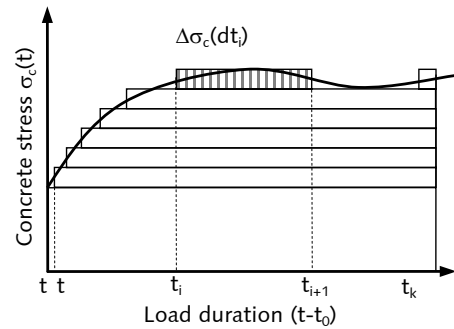


Fig. 1: Discretization of concrete stress history into stress increments $\Delta\sigma_c$

the short-term creep compliance which is included in the experimental determination of Young's modulus. The total strain is calculated using Eq. (5).

B. Application of Models to Varying Stresses

The creep models described in the latter section are valid only for constant stresses, which is a special case that does not occur in reinforced concrete, prestressed concrete, or steel-concrete-composite structures. Caused by the bond of the materials steel and concrete a permanent redistribution of stresses takes place so that the case of constant stress is not practically relevant. Hence, the approaches explained in the last section need to be modified into integral or differential formulations in order to simulate variable stresses.

Assuming linear creep, the superposition principle for linear visco-elastic materials from Boltzmann [2] can be applied. This principle takes into account the loading and deformational states for different beginnings of loading or durations of loading. Hence, it is possible to consider the explicit loading history of concrete when calculating the creep strains [12]. The stress history is unknown in advance so that a direct integration of the stresses over time is impossible. Thus, a numerical calculation of the creep strains is necessary. The stress history is divided into stress increments $\Delta\sigma_c$, Fig. 1, and the total displacement at time t results from the sum over all N increments

$$\varepsilon_{c,tot} = \sigma_c(t_0) J_c(t, t_0) + \sum_{i=1}^N \Delta\sigma_c(t_i) J_c(t, t_i), \quad (10)$$

with the actual time increment i , the time at beginning of an increment t_i , and its corresponding stress increment $\Delta\sigma_c(t_i)$. In case of non-linear creep the extension of this method by Diener [3] can be applied. In order to calculate the creep strains at the actual time t the superposition principle requires the summation over all previous time-steps which is, especially for large structures, a time and computer-power demanding procedure. Hence, different simplifications of the superposition principle were developed to reduce the computational effort.

The simplest but most uncertain method is the Effective Modulus Method (EMM). The compliance at time t is simply

increased by the creep coefficient

$$J_c(t, t_0) = \frac{1 + \varphi_c(t, t_0)}{E_c}, \quad (11)$$

and the total strain is calculated according to Eq. (5). The stress history is not considered and only the stress at time t causes creep deformations. Due to effects of redistribution at cross-section level are these stresses always lower than at beginning of loading, thus, the creep deformations are underestimated. Nevertheless, due to its simplicity this method is used quite often for practical applications.

A further simplification of the time-integration is the procedure according to Trost [12], also known as Age-Adjusted Effective Modulus Method (AAEMM) established by Bažant [13]. Assuming a time-independent elastic modulus and introducing the aging coefficient $\rho_c(t, t_0)$ the total strain becomes

$$\begin{aligned} \varepsilon_{c,tot}(t, t_0) &= \frac{\sigma_c(t_0)}{E_c} [1 + \varphi_c(t, t_0)] \\ &+ \frac{1}{E_c} [\sigma_c(t) - \sigma_c(t_0)] [1 + \rho_c(t, t_0) \varphi_c(t, t_0)]. \end{aligned} \quad (12)$$

The influence of aging of concrete on the creep behavior in case of varying stresses for times $t > t_0$ is described by the aging coefficient. Many theoretical work has been performed to calculate the aging coefficient. Analyzing the limit values reveals that the aging coefficient is in the range of $0.5 \leq \rho_c(t, t_0) \leq 1.0$. The value of $\rho_c(t, t_0) = 1.0$ characterizes the lower limit of the creep deformations so that this method becomes similar to the Effective Modulus Method. In case of $\rho_c(t, t_0) = 0.5$ the creep strains are maximal. For reasons of simplification, TROST proposes to assume $\rho_c(t, t_0) = 0.8$, which was also confirmed by the work of Blesensohl [14] and which is used for most practice applications.

III. METHOD OF SENSITIVITY ANALYSIS

Sensitivity analyses are a widely-used tool to apportion the model output uncertainty to the model input parameters [15], for example which material parameters mainly affect the uncertainty of a stress-strain-relation of a constitutive model. Most [16] extended the existing concepts to study the influence of model selection on the output. In other words, apart from the output variation originating from uncertain input parameters the uncertainty coming from varying models is taken into account, knowing that none of these models is perfect for the description of a particular phenomenon. This idea is extended in this paper and the influence of the model selection as well as the influence of the chosen time-integration on the models' prognoses is investigated by means of sensitivity analyses.

For this purpose variance based global sensitivity analyses following the concept of Saltelli et al. [15] are applied. It is assumed that a model output Y is a function depending on a set of input parameters \mathbf{X} , $Y = f(X_1, X_2, \dots, X_n)$. The surveys are generally divided into the calculation of first-order S_i and total-effects S_{T_i} sensitivity indices. The first-order sensitivity

index S_i [17] describes the exclusive influence of parameter X_i on the model response and is determined with

$$S_i = \frac{V_{X_i}(E_{X_{\sim i}}(Y|X_i))}{V(Y)} = 1 - \frac{E_{X_i}(V_{X_{\sim i}}(Y|X_i))}{V(Y)}. \quad (13)$$

Herein, $V_{X_i}(E_{X_{\sim i}}(Y|X_i))$ is the variance of the model response Y due to the variation of X_i and $V(Y)$ is the variance of the system response when all parameters vary simultaneously. Further, $E_{X_i}(V_{X_{\sim i}}(Y|X_i))$ is the expected value of the variance when all parameters but X_i vary, denoted as $X_{\sim i}$. If the sum of all S_i is close to one, the model is additive, no interaction of the parameters exist. A $\sum S_i < 1$ means that some parts of the variance cannot be explained when the interaction of the parameters is neglected.

In order to take into account coupling effects, the total-effects sensitivity index S_{T_i} was introduced [18]

$$S_{T_i} = 1 - \frac{V(E(Y|X_{\sim i}))}{V(Y)} = \frac{E(V(Y|X_{\sim i}))}{V(Y)}, \quad (14)$$

with the expected value of the variance $E(V(Y|X_{\sim i}))$ and the variance $V(E(Y|X_{\sim i}))$ for the case that all parameters but X_i itself vary. Besides the exclusive influence of the parameter X_i on the variance of the response, the S_{T_i} index considers the interaction of X_i with further parameters $X_{\sim i}$. In general, the numerical calculation of these indices requires a special sampling procedure with a subsequent stochastic analysis, explained in detail in [15].

Here, the sensitivity analysis is applied to study the influence of model selection and choice of the time-integration on the resulting time-dependent deformations. Instead of the sensitivity of the output to model parameters, the sensitivity of the output to model selection M and time-integration I is determined. Two uncorrelated, uniformly distributed, discrete random parameter X_M and X_I are introduced

$$X_M \in \{1, 2, \dots, n_M\} \text{ and } X_I \in \{1, 2, \dots, n_I\}, \quad (15)$$

wherein the possible values of X_M denote the choice of one of the n_M creep models and the possible values of X_I account for one of the n_I time-integration method. For these two random variables the sensitivity indices are calculated. Due to the fact that discrete parameters are considered, a finite number of possible parameter combinations n_{comb} exists

$$n_{comb} = n_M \cdot n_I. \quad (16)$$

Hence, the terms $V(E(Y|X_i))$, $V(E(Y|X_{\sim i}))$, and $V(Y)$ in Eq. (13) and (14) can be calculated directly and exactly without the need for the full sensitivity scheme by Saltelli.

The resulting total-effects indices $S_{T_i}^M$ and $S_{T_i}^I$ indicate the influence of the model selection and choice of time-integration on the model output. The greater an index, the higher the influence of the parameter, for example a high $S_{T_i}^M$ and a low $S_{T_i}^I$ symbolize that the selection of an appropriate creep model is of higher importance for the model response than the choice of the time-integration method. In case of the time-dependent behavior of creep the resulting sensitivity indices are also time-dependent.

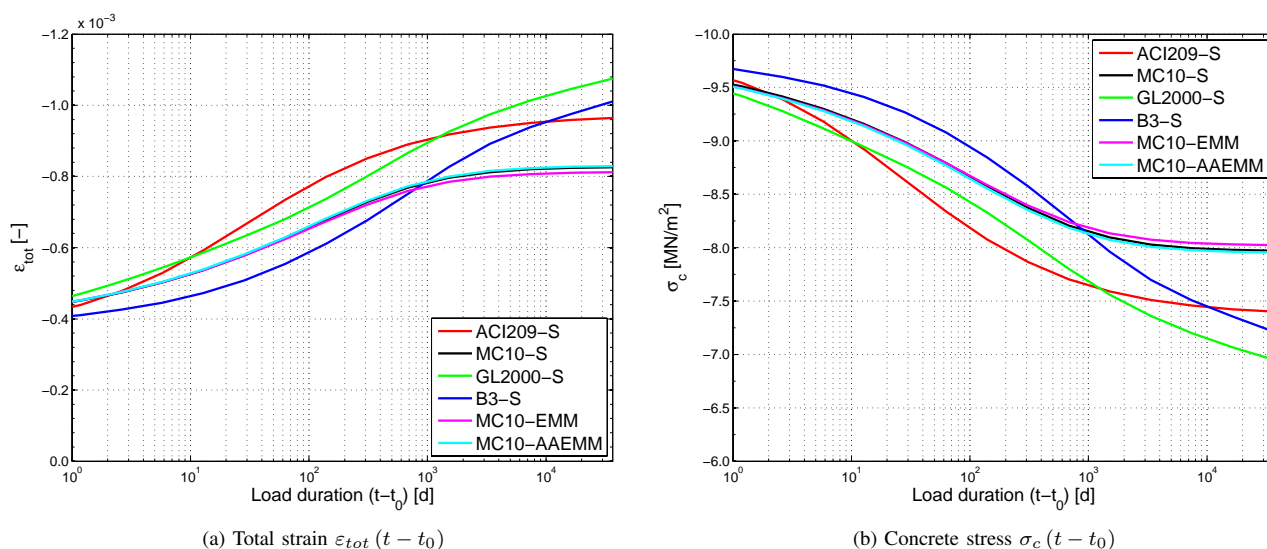


Fig. 2: Time-dependent concrete strains and stresses for various models and time-integration methods, $\rho = 2.0\%$, $t_0 = 28$ d, neglect post-hardening

TABLE I: Material, model and environmental input parameters

parameter	value	model
RH	65 %	ACI209, MC10, B3, GL2000
$f_{c,28}$	38 MN/m^2	MC10, B3
$E_{c0,28}$	31900 MN/m^2	MC10
$E_{cm,28}$	27150 MN/m^2	ACI209, GL2000
c	362 kg/m^3	B3
w/c	0.47	B3
a/c	5.16	B3
$f - a$	0.50	ACI209
sl	38 cm	ACI209
a	0.015	ACI209
k_s	1.15	B3
E_s	200000 MN/m^2	-

IV. NUMERICAL EXAMPLE

A. Geometry, Material Properties and Preliminary Results

The effect of the application of different creep models and different time-integration methods on the time-dependent response is demonstrated using the example of a rectangular reinforced concrete cross-section with a width and a height of $w = h = 30$ cm. The material considered is concrete C30/37 combined with reinforcing steel B500B, distributed symmetrical around the cross-section. The sensitivity analyses are performed for different degrees of reinforcement, varying from $\rho = 0.0\%$ up to $\rho = 9.0\%$. The output quantity is the total strain of the cross-section ε_{tot} , equivalent to the total concrete strain $\varepsilon_{c,tot}$, under a time-independent constant compressive force of $F = -1000$ kN. The material properties of concrete and further boundary conditions are given in Tab. I. Further parameters are: concrete age at beginning of drying $t_d = 7$ d, temperature $T = 20$ C, and cement type CEM II 42.5N.

To give a primarily impression of the effects of different creep models and time-integration methods, Fig. 2 depicts

the time-dependent total strains ε_{tot} and concrete stresses σ_c for the given cross-section. In this case the degree of reinforcement is fixed to $\rho = 2.0\%$, the concrete age at beginning of loading is chosen to $t_0 = 28$ d and post-hardening is neglected. The abbreviations used in the legend of the figure are the different identifiers of the creep models, ACI209, MC10, GL2000, and B3, as well as the method of time-integration, S for Superposition according to Boltzmann, EMM for the Effective Modulus Method, and AAEMM for the Age-Adjusted Effective Modulus Method. At the first glance large discrepancies for the different model/integration combinations are visible. Analyzing the total strains, Fig. 2a, a range from $\varepsilon_{tot} \approx -0.80\text{E-}3$ up to $\varepsilon_{tot} \approx -1.08\text{E-}3$ is observed for a load duration of 100 years. On a closer look it becomes obvious that the different choice of one of the four creep models leads to larger variations, $-0.83\text{E-}3 \leq \varepsilon_{tot} \leq -1.08\text{E-}3$, than the choice of the different integration methods, $-0.80\text{E-}3 \leq \varepsilon_{tot} \leq -0.83\text{E-}3$. Whereas the variation of the different creep models is high for all load durations, the differences within the integration methods require a certain time to emerge. This fact is explained with the continuous decrease of concrete stresses due to the redistribution of stresses at cross-section level. As the stress differences from the beginning of loading t_0 to the actual time t increase, the significance of the time-integration method increases simultaneously. Similar results are observed when the concrete stresses σ_c are studied, Fig. 2b.

B. Results of Sensitivity Analysis

The results shown in Fig. 2 characterize only one sample for the different influence of model selection and time-integration. In order to achieve general valid results and to quantify the importance of the model/integration, different degrees of reinforcement need to be investigated in the framework of

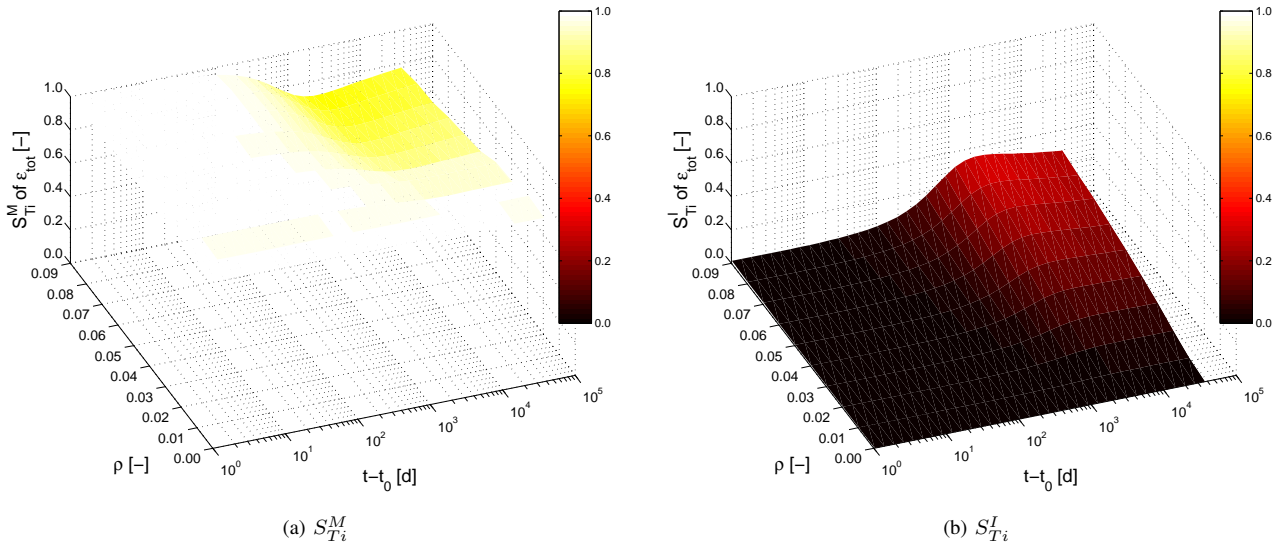


Fig. 3: S_{T_i} of total strain ε_{tot} , $t_0 = 28$ d, neglect of post-hardening

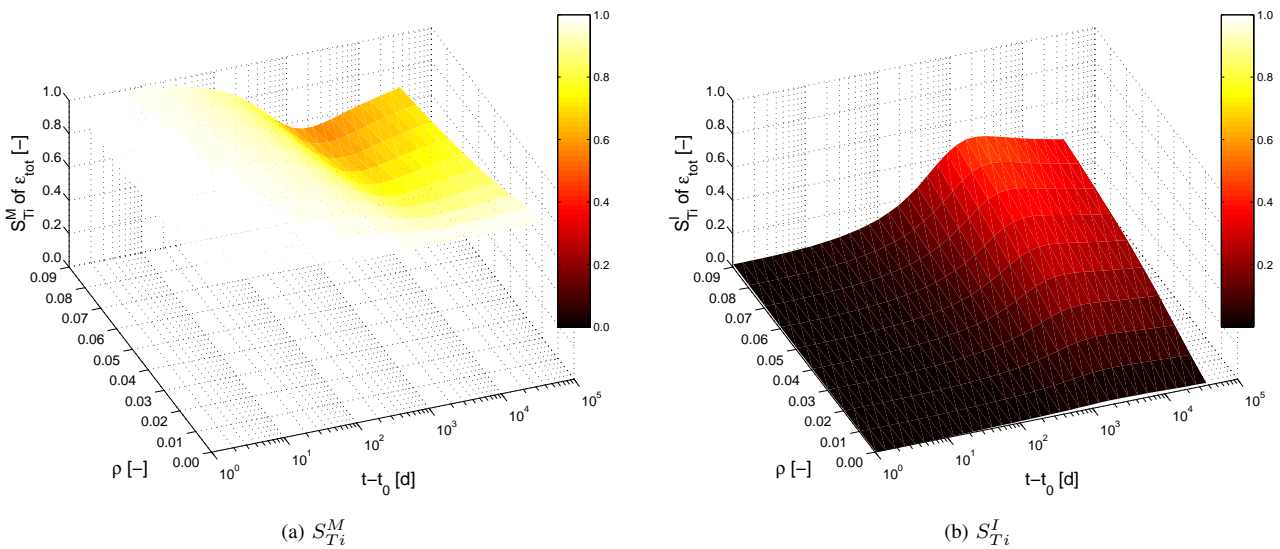


Fig. 4: S_{T_i} of total strain ε_{tot} , $t_0 = 28$ d, including post-hardening

global sensitivity analysis, which will be presented in this section. The method of sensitivity analysis described in section III is applied to the example of the rectangular reinforced concrete cross-section. The sensitivity analyses are performed for different scenarios. First, it is distinguished between the consideration and neglect of post-hardening of concrete. Second, two different ages of concrete at beginning of loading are taken into account, $t_0 = 28$ d and $t_0 = 7$ d. Post-hardening of concrete is simulated using the model according to MC10 [7]. If post-hardening is combined with the superposition principle of Boltzmann, the stresses of concrete need to be calculated by time-integration as well, for details see [1].

The resulting total-effects sensitivity indices for model selection $S_{T_i}^M$ and choice of the time-integration method $S_{T_i}^I$

are depicted in Figs. 3–6 for the different scenarios depending on the degree of reinforcement ρ and load duration. The index S_{T_i} quantifies the influence of M and I taking into account interactions between the selection of creep model and the choice of time-integration method.

Analyzing Fig. 3, which depicts the results considering $t_0 = 28$ d and neglects post-hardening, a high importance of the creep model selection is observed with $S_{T_i}^M \geq 0.80$. In contrast to this value, the sensitivity towards the choice of the time-integration is small $S_{T_i}^I \leq 0.30$. A general increase of $S_{T_i}^I$ with an increasing load duration is recognized, what can be explained with larger differences of concrete stresses when creep strains increase for higher load durations. Further, Fig. 3 points out that the influence of time-integration increases with

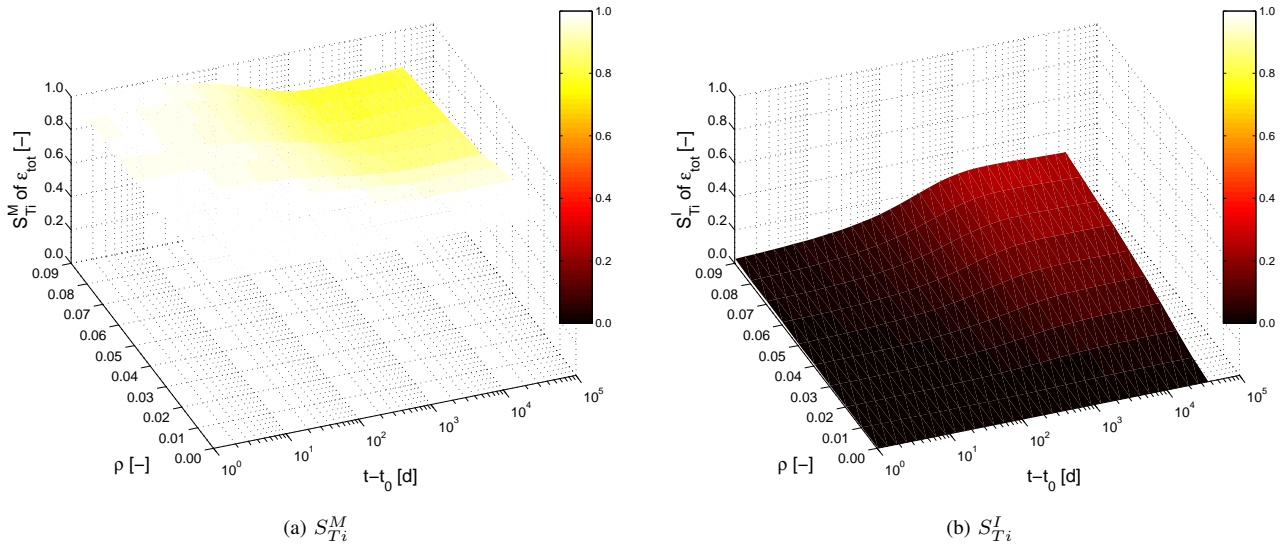


Fig. 5: S_{T_i} of total strain ε_{tot} , $t_0 = 28$ d, neglect of post-hardening

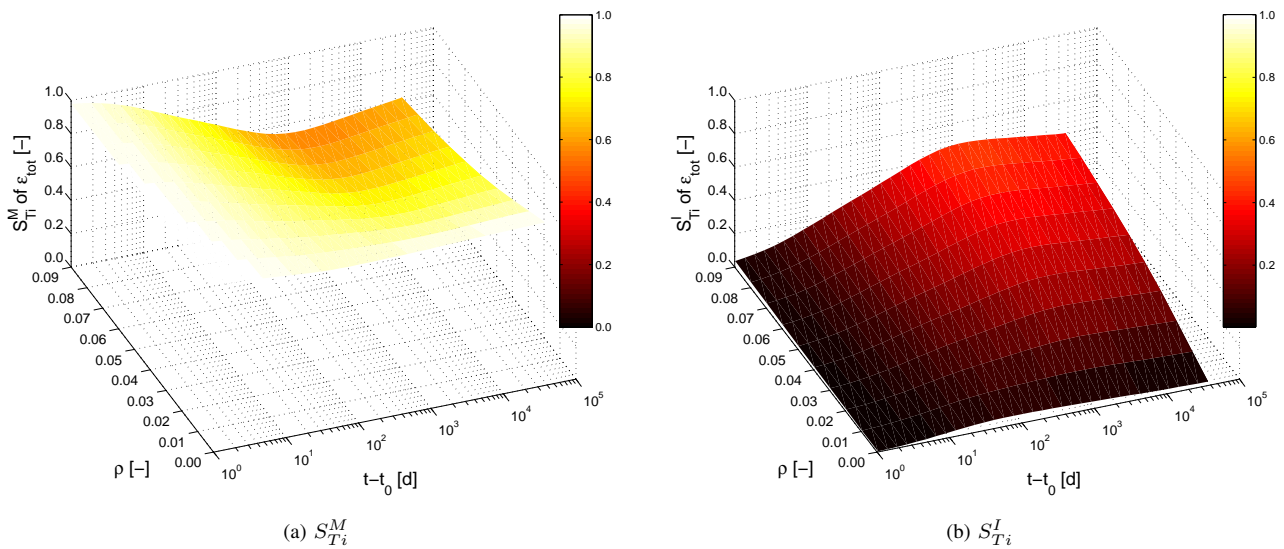


Fig. 6: S_{T_i} of total strain ε_{tot} , $t_0 = 28$ d, including post-hardening

an increasing degree of reinforcement as the redistribution of stresses at cross-section level is more pronounced. The more redistribution of stresses, the larger the stress differences of concrete and the higher the effects of choosing different time-integration method. For $\rho = 0.0\%$ the index $S_{T_i}^I$ is equal to zero, which results from the constant concrete stress that occurs in this case. Consequently, no time-integration is required.

The degrees of reinforcement considered in the scope of this paper are generally high going up to $\rho = 9.0\%$. For ordinary RC structures ρ is less than 3.0% , which results to a maximum of $S_{T_i}^I \approx 0.15$. Hence, the selection of creep models is much more important for practical applications. The small increase of $S_{T_i}^M$ for $t - t_0 \geq 1000$ d originates from the

increasing variation of the creep prognoses of the four models for these large load durations, because the models differ in the main assumption of long-term creep behavior: models ACI209 and MC10 assume an ultimate creep coefficient, equivalent to a finite creep compliance, and models GL2000 and B3 postulate a continuous increase of creep compliance.

The same comparison of sensitivity indices is made in Fig. 4, but this time additionally post-hardening of concrete is taken into account. The general findings are similar to the latter stanza, but small differences occur. Due to the post-hardening the impact of the time-integration is more pronounced, thus the total-effects sensitivity index increases up to $S_{T_i}^I \approx 0.4$ for very high degrees of reinforcement. Furthermore, in contrast to the previous figure even without reinforcement, $\rho = 0.0\%$,

a small $S_{T_i}^I$ is observed. This difference is caused by the Effective Modulus Method, which does not consider any stress history and which defines the strains at time t depending on the actual Young's modulus of concrete $E_{c,t}$ instead of the Young's modulus at beginning of loading E_{c,t_0} .

The sensitivity indices for a concrete loaded at $t_0 = 7$ d are depicted in Figs. 5 and 6. In comparison to $t_0 = 28$ d a higher $S_{T_i}^I$ occurs even for smaller load durations of $t - t_0 = 10$ d...100 d, thus, the importance of the time-integration method increases. This finding arises from the larger creep affinity of concrete when loaded in the early ages, which results in a stronger stress redistribution requiring an adequate time-integration method. Further, the effect of post-hardening is more pronounced for $t_0 = 7$ d than for $t_0 = 28$ d as the post-hardening of this young concrete is much higher than for an elder concrete. Nevertheless, the influence of the model selection is dominating against the influence of the choice of time-integration method if the degree of reinforcement is within practical relevant limits of $\rho \leq 3.0\%$, quantified by values of $S_{T_i}^M \geq 0.80$.

V. CONCLUSION

The presented method of sensitivity analysis points out the main influential parameter on the output uncertainty of creep models - parameter in this case is understood as the selection of creep models or the choice of time-integration methods. The methodology is generally formulated and can be applied to further problems of model selection or analysis methods.

The results of the numerical example show that the uncertainty of creep prediction for varying stresses originates rather from the selection of creep models than from the choice of time-integration methods. With increasing degree of reinforcement, increasing load duration, and the consideration of post-hardening the influence of the time-integration method increases, but it is still lower in comparison to the impact of the various creep models. For practical relevant degrees of reinforcement of $\rho \leq 3.0\%$ the influence of creep model selection on the output uncertainty is much higher ($S_{T_i}^M \geq 0.80$) than the influence of different time-integration methods ($S_{T_i}^I \leq 0.25$). Hence, future focus of practical engineers should be more on the identification and subsequent selection of the most appropriate creep model using evaluation methods for their prediction quality [5] than wasting modeling and computational effort by choosing a more sophisticated time-integration method.

APPENDIX

The following symbols are used:

TABLE II: Notations

symbol	meaning
a	void volume of concrete [-]
a/c	aggregate-cement-ratio [-]
$\beta...$	correction factors [-]
C_c	creep compliance [m^2/MN]
C_0	basic creep compliance [m^2/MN]

symbol	meaning
C_d	drying creep compliance [m^2/MN]
c	cement content [kg/m^3]
d	addend of time-function [d]
$E(...)$	expected value
$E_{c,0}, E_{cm}$	tangent and secant stiffness of concrete [MN/m^2]
$E_{c,t}$	stiffness of concrete at time t [MN/m^2]
E_s	Young's modulus of steel [MN/m^2]
ε_{tot}	total strain [-]
$\varepsilon_{c,cr}$	creep strain of concrete [-]
$\varepsilon_{c,tot}$	total strain of concrete [-]
φ_c	creep coefficient [-]
$\varphi_{c,\infty}$	ultimate creep coefficient [-]
$\phi(t_c)$	factor considering drying before loading [-]
f_{cm}	mean compressive concrete strength [MN/m^2]
$F_{\Omega}(\sigma_c)$	over-proportionality factor [-]
$f-a$	fine-aggregate-ratio [-]
$\gamma...$	correction factors [-]
I	index for choice of time-integration
J_c	total compliance of concrete [m^2/MN]
M	index for model selection
N	number of time increments [-]
n_{comb}	number of model combinations [-]
n_I	number of time-integration methods [-]
n_M	number of creep models [-]
Ψ	exponent of time-function [-]
$q...$	individual compliances [m^2/MN]
RH	relative humidity [-]
ρ	degree of reinforcement [-]
ρ_c	aging coefficient [-]
S_i, S_{T_i}	first-order and total-effects sensitivity index [-]
σ_c	concrete stress [MN/m^2]
$\Delta\sigma_c$	stress increment [MN/m^2]
sl	slump [cm]
T	temperature [C]
t, t_d, t_0	actual time, time at beginning of drying and loading [d]
$V(...)$	variance
V/S	volume-surface-ratio
w/c	water-cement-ratio [-]
\mathbf{X}	vector of input parameters
X_i^M	discrete parameter to select creep model [-]
X_i^I	discrete parameter to select time-integration method [-]
Y	model response

ACKNOWLEDGMENT

This research is supported by the German Research Institute (DFG) via Research Training Group "Evaluation of Coupled Numerical Partial Models in Structural Engineering (GRK 1462)", which is gratefully acknowledged by the authors.

REFERENCES

- [1] R. Gilbert, *Time Effects in Concrete Structures*. Elsevier, 1988.
- [2] L. Boltzmann, "Zur Theorie der elastischen Nachwirkung," *Annalen der Physik und Chemie*, vol. 7, pp. 624-654, 1876.
- [3] J. Diener, "Beitrag zur physikalisch und geometrisch nichtlinearen Berechnung langzeitbelasteter Bauteile aus Stahlbeton und Spannbeton unter besonderer Berücksichtigung des nichtlinearen Kriechens und der Rissbildung," Dissertation, Bauhaus-Universität Weimar, 1998.
- [4] I. Wallmichrath, "Ein Beitrag zur wirklichkeitsnahen Berechnung schlanker Stahlbetonrahmen," Dissertation, Technische-Universität Hamburg-Harburg, 2007.

- [5] H. Keitel, "Bewertungsmethoden für die Prognosequalität von Kriechmodellen des Betons - Evaluation Methods for Prediction Quality of Concrete Creep Models," Dissertation, Bauhaus-Universität Weimar, 2011.
- [6] ACI209, "Prediction of Creep, Shrinkage, and Temperature Effects in Concrete Structures," American Concrete Institute, Tech. Rep., 1992.
- [7] International Federation for Structural Concrete (fib), "fib Model Code 2010 - First Complete Draft - Volume 1," International Federation for Structural Concrete (fib), Tech. Rep., 2010.
- [8] N. Gardner and M. Lockman, "Design Provisions for Drying Shrinkage and Creep of Normal-Strength Concrete," *ACI Materials Journal*, vol. 98, pp. 159–167, 2001.
- [9] Z. Bažant and S. Bajewa, "Creep and Shrinkage Prediction Model for Analysis and Design of Concrete Structures - Model B3," *Materials and Structures*, vol. 28, pp. 357–365, 1995.
- [10] Z. Bažant and S. Prasanna, "Solidification Theory for Concrete Creep. I: Formulation," *Journal of Engineering Mechanics*, vol. 115, pp. 1691–1703, 1989.
- [11] Z. Bažant and S. Prasanna, "Solidification Theory for Concrete Creep. II: Verification and Application," *Journal of Engineering Mechanics*, vol. 115 (8), pp. 1704–1725, 1989.
- [12] H. Trost, "Auswirkungen des Superpositionsprinzips auf Kriech- und Relaxationsprobleme bei Beton- und Spannbeton," *Beton - und Stahlbetonbau*, vol. 62, pp. 230–238 & 261–269, 1967.
- [13] Z. Bažant, "Prediction of Concrete Creep Effects Using Age-Adjusted Effective Modulus Method," *ACI Journal*, vol. 69, pp. 212–217, 1972.
- [14] B. Blessenohl, "Zur numerischen Berechnung der Auswirkungen des Kriechens und Schwindens auf Betonverbundtragwerke - Grundlagen und Algorithmen für die EDV," Dissertation, Rhein-Westfälische Technische Hochschule Aachen, 1990.
- [15] A. Saltelli, M. Ratto, T. Andres, F. Campolongo, J. Cariboni, D. Gatelli, M. Saisana, and S. Tarantola, *Global Sensitivity Analysis. The Primer*. John Wiley and Sons, 2008.
- [16] T. Most, "Assessment of Structural Simulation Models by Estimating Uncertainties due to Model Selection and Model Simplification," *Computers and Structures*, vol. 89, pp. 1664–1672, 2011.
- [17] I. M. Sobol, "Sensitivity Estimates for Nonlinear Mathematical Models," *Mathematical Modeling & Computational Experiment*, vol. 1, pp. 407–414, 1993.
- [18] T. Homma and A. Saltelli, "Importance Measures in Global Sensitivity Analysis of Nonlinear Models," *Reliability Engineering and System Safety*, vol. 52, pp. 1–17, 1996.